Critical Neutron Scattering in $SrTiO_3$ and $KMnF_3$ †

S. M. Shapiro, J. D. Axe, and G. Shirane
Brookhaven National Laboratory, Upton, New York 11973

and

T. Riste*
Institutt for Atomenergi, Kjeller, Norway
(Received 21 June 1972)

The accepted view of the dynamics of the structural phase transition in $SrTiO_3$ ($T_c \sim 100$ °K) and $KMnF_3$ ($T_c \sim 186$ °K) had been that of a soft zone-boundary ($\vec{q} = \vec{q}_R$) phonon driving the transition with a frequency ω_∞ that goes to zero as $T \to T_c$ from above. Recently, Riste *et al.* observed in the neutron-scattering spectra of $SrTiO_3$ a temperature-dependent central component centered around $\omega = 0$ and $\vec{q} = \vec{q}_R$ in addition to the phonon sidebands centered around $\omega = \omega_\infty$. We report on higher-resolution neutron studies of the central component and sidebands in $SrTiO_3$, as well as the observation of a central peak in $KMnF_3$. The central component is interpreted as arising from a low-frequency resonance in the self-energy of the soft mode and is characterized by a frequency ω_0 related to ω_∞ by the anharmonic coupling constant δ, $\omega_0^2 = \omega_\infty^2 - \delta^2$. The temperature behavior of the $SrTiO_3$ spectra as T decreases shows a rapid increase in the intensity of the central component as the sideband frequency ω_∞ decreases. Near T_c, the intensity of the central peak diverges and ω_∞ approaches a finite limiting value. Since ω_0^{-2} is proportional to the total intensity, the diverging intensity implies that $\omega_0 \to 0$ as $T \to T_c$. It is shown that the temperature dependence of ω_0^2 is stronger than that predicted from mean-field theory. The energy width of the central component is < 0.02 meV and we observe a narrow temperature-dependent q width. In $KMnF_3$, the central component is clearly seen even though the soft phonons are already overdamped at 40 °K from T_c. The observed spectra have a similar behavior with decreasing temperature as studied in $SrTiO_3$.

I. INTRODUCTION

Over the past decade structural phase transitions have been extensively studied. One of the largest classes of crystals studied which undergoes structural phase transitions is crystals of the perovskite structure, which have high-temperature cubic phases transforming as the temperature is reduced into a lower-symmetry tetragonal or trigonal phase.[1] It is generally accepted that the phase transition is driven by a normal vibrational mode of the lattice whose atomic displacements are those necessary to take the crystal from one symmetry class to the other.[2] In simplest terms, the frequency of this mode is thought to decrease toward zero as $T \to T_c$, and at T_c the restoring forces for this particular vibrational mode vanish and the atoms easily shift to the new equilibrium positions commensurate with the change in symmetry. This "soft-mode" concept has been most useful in explaining anomalies in the temperature dependence of various macroscopic properties and in providing an understanding of the mechanism of structural phase transitions.

In some perovskites ($BaTiO_3$, $KTaO_3$, $KNbO_3$) the soft mode is a zone-center vibration and in others ($SrTiO_3$, $KMnF_3$, $LaAlO_3$) the soft mode occurs at the $R = \frac{1}{2}\frac{1}{2}\frac{1}{2}$ point of the Brillouin zone.[1] In several perovksites ($SrTiO_3$, $LTaO_3$, $LaAlO_3$) the soft mode remains underdamped to within a few degrees of the transition temperature, whereas in others ($BaTiO_3$, $KMnF_3$, $KNbO_3$) it is already overdamped far from T_c.[1] The response functions of the underdamped and the overdamped cases differ in that in the former there are two resonant peaks corresponding to creation and annihilation of the phonon and in the latter the two peaks have merged into one broad peak centered around $E = 0$.

The application of the soft-mode picture to the transition in $SrTiO_3$ was first discussed in detail by Fleury, Scott, and Worlock.[3] In the cubic phase the displacements of the soft mode transform according to the triply degenerate Γ_{25} representation of the group of R and correspond to rotation of the oxygen tetrahedra about the $\langle 100 \rangle$ axes. At T_c there is a doubling of the unit cell and the zone boundary of the cubic phase now becomes the zone center of the tetragonal phase. The triply degenerate zone-boundary Γ_{25} mode of the cubic phase splits into two zone-center modes: a doublet with rotation axes perpendicular to the fourfold axis and a singlet with rotation axis parallel to the fourfold axis. In their Raman study of the tetragonal phase, Fleury *et al.* observed two modes whose frequency approached zero as $T \to T_c$. Shirane and Yamada[4] confirmed the model in a neutron-scattering study of the cubic phase where they observed a soft mode at the R point of the Brillouin zone.

Prior to last year, it was believed that the order parameter and frequency of the soft mode in

$SrTiO_3$ differed little from the mean-field or classical picture of structural phase transitions. Recently there have been new observations on $SrTiO_3$ which indicate substantial deviation from mean-field behavior. Müller and Berlinger[5] measured the order parameter (i.e., the rotational displacements) by electron paramagnetic resonance (EPR) in iron-doped $SrTiO_3$ below the transition temperature and found a temperature dependence $(T - T_c)^{\beta}$ with $\beta = 0.33 \pm 0.02$ within the critical region of $T_c - T < 10\ ^{\circ}K$.

Riste, Samuelsen, Otnes, and Feder,[6] in their neutron-scattering studies of the soft phonon in $SrTiO_3$, observed a "central component," centered around energy $\omega = 0$ and $\vec{q} = \vec{q}_R$, whose intensity diverged as the transition temperature was approached from above. It is this critical scattering and its temperature dependence that we shall discuss below.[7]

$KMnF_3$ shows a similar cubic-to-tetragonal phase transformation with two striking differences. The phonon branch from the R to M point in the Brillouin zone has an anomalously low frequency[8] which has explained the diffuse streaks observed in x-ray experiments.[9] In addition, the soft mode at the R point is already highly overdamped at 40 °K from the transition temperature $T_c = 186\ ^{\circ}K$.[10] Gesi *et al.* studied in detail the temperature dependence of the soft mode.[8] By fitting their data to the simple damped-harmonic-oscillator model, they found an unexpected temperature-dependent behavior of the soft-mode damping. This led to our present high-resolution reinvestigation of $KMnF_3$ and the observation of a narrow central peak in addition to the overdamped phonon peak.

II. THEORY

The suggestion that a soft phonon mode might develop a three-peaked spectral response was first made by Tani.[11] Cowley[12] specifically showed that a three-peaked function can be present in the spectral response of a piezoelectric crystal. Briefly, the basic ideas of the latter suggestion can be described as follows: The frequency spectrum of the fluctuations in a given jth branch of the lattice is given in anharmonic perturbation theory as[13]

$$S(\vec{q}, \omega) = \frac{1}{\pi}\,[n(\omega)+1]\,\mathrm{Im}[\Omega^2(\vec{q}) + \Pi(\vec{q}, \omega, T) - \omega^2]^{-1}\,, \tag{1}$$

where $n(\omega) = (e^{\omega/kT} - 1)^{-1}$ is the phonon occupation number (ω is given in energy units) and $\Omega(\vec{q})$ is the $\vec{q}$-dependent harmonic frequency. The imaginary part of the anharmonic self-energy, $\mathrm{Im}\Pi(\vec{q}, \omega, T)$, includes the effects of real scattering processes which limit the lifetime of the state $\vec{q}$, and $\mathrm{Re}\Pi(\vec{q}, \omega, T)$ renormalizes the harmonic frequency and allows for a temperature-dependent quasiharmonic frequency.

Let us now assume the following form[14] for $\Pi(\vec{q}, \omega, T)$:

$$\Pi(\vec{q}, \omega, T) = [\Delta(\vec{q}, T) - i\omega\Gamma_0(T)] - \frac{\gamma\delta^2(T)}{\gamma - i\omega}\,. \tag{2}$$

The shift and broadening associated with the terms in square brackets represent interactions with multiphonon excitations which can be regarded as frequency-independent quantities because the multiphonon states have a wide characteristic-frequency distribution (of the order ω_{Debye}). The physical idea which forms the motivation of the last term is the postulated existence of an additional channel for decay [with a coupling constant proportional to $\delta^2(T)$] of those phonon fluctuations with frequencies ω less than some characteristic frequency γ. We postpone, for the moment, further discussion of the detailed nature of this low-frequency decay channel.

Substituting (2) into (1) we get

$$S(\vec{q}, \omega) = \frac{1}{\pi}\,[n(\omega)+1]\,\mathrm{Im}\left[\left(\omega_\infty^2(\vec{q}, T) - \frac{\delta^2(T)\gamma^2}{\omega^2+\gamma^2} - \omega^2\right) + i\omega\left(\Gamma_0 + \frac{\delta^2(T)\gamma}{\omega^2+\gamma^2}\right)\right]^{-1}\,, \tag{3}$$

where the quasiharmonic frequency $\omega_\infty^2(\vec{q}, T) = \Omega^2(\vec{q}) + \Delta(T)$ results from renormalization due to the virtual scattering with multiphonon states and is slowly varying with frequency.

If we use the high-temperature limit $n(\omega) = k_B T/\omega \gg 1$, Eq. (3) becomes

$$S(\vec{q}, \omega) = \frac{k_B T}{\pi}\,\frac{\Gamma_0 + [\delta^2(T)\gamma/(\omega^2+\gamma^2)]}{\{\omega_\infty^2(\vec{q}, T) - [\delta^2(T)\gamma^2/(\omega^2+\gamma^2)] - \omega^2\}^2 + \omega^2\{\Gamma_0 + [\delta^2(T)\gamma/(\omega^2+\gamma^2)]\}^2}\,. \tag{4}$$

Equation (4) obeys the following sum rule:

$$\int_{-\infty}^{+\infty} S(\vec{q}, \omega)\,d\omega = \frac{k_B T}{\omega_\infty^2(\vec{q}, T) - \delta^2(T)} = \frac{k_B T}{\omega_0^2(\vec{q}, T)}\,, \tag{5}$$

where $\omega_0^2(\vec{q}, T) \equiv \omega_\infty^2(\vec{q}, T) - \delta(T)^2$ is the square of the renormalized mode frequency in the limit $\omega \to 0$.

The manner in which the structure in the self-energy $\Pi(\vec{q}, \omega, T)$ is reflected in $S(\vec{q}, \omega)$ can be most clearly demonstrated if $\Gamma_0 \ll \delta^2/\gamma$ and $\omega_\infty^2 \gg \gamma$. Then Eq. (4) can be separated into two terms $S(\vec{q}, \omega) = S(\vec{q}, \omega)_{\mathrm{cent}} + S(\vec{q}, \omega)_{\mathrm{side}}$, where

$$S(\vec{q}, \omega)_{\mathrm{cent}} = \frac{k_B T}{\pi}\,\frac{\delta^2(T)}{\omega_0^2(\vec{q}, T)\omega_\infty^2(\vec{q}, T)}\,\frac{\gamma'^2}{\omega^2+\gamma'^2} \tag{6}$$

is a narrow Lorentzian of width $\gamma' = \gamma(\omega_0^2/\omega_\infty^2)$ centered about $\omega = 0$ and

$$S(\vec{q}, \omega)_{\text{side}} = \frac{k_B T}{\pi} \frac{\Gamma_0}{[\omega_\infty^2(\vec{q}, T) - \omega^2]^2 + \omega^2 \Gamma_0^2} \tag{7}$$

is the familiar damped-harmonic-oscillator response with characteristic frequencies $\pm\omega_\infty(\vec{q}, T)$. By integrating (6) and (7) we see how they contribute separately to the sum rule (5):

$$\int S(\vec{q}, \omega)\, d\omega = \int S(\vec{q}, \omega)_{\text{cent}}\, d\omega + \int S(\vec{q}, \omega)_{\text{side}}\, d\omega ,$$

$$\frac{1}{\omega_0^2(\vec{q}, T)} = \frac{\delta^2(T)}{\omega_0^2(\vec{q}, T)\omega_\infty^2(\vec{q}, T)} + \frac{1}{\omega_\infty^2(\vec{q}, T)} . \tag{8}$$

It is easy to see from Eq. (8) how such a spectral response would modify the usual soft-mode picture of a lattice instability. As the instability is approached from higher temperatures $\omega_\infty^2(\vec{q}, T)$ decreases with a corresponding increase in the intensity of the "phononlike" sidebands $[\sim 1/\omega_\infty^2(\vec{q}, T)]$. But the intensity in the central component increases even more rapidly $[\sim 1/\omega_\infty^4(\vec{q}, T)$ for $\omega_\infty^2 \gg \delta^2]$, and the divergent fluctuations (critical scattering) which characterize the instability occur in this central component. Furthermore, the lattice instability occurs when $\omega_0(0, T_c) \to 0$, not when $\omega_\infty(0, T_c) \to 0$. Thus at T_c, $\omega_\infty^2(0, T_c) = \delta^2(T_c)$ and is nonzero provided $\delta^2(T_c)$ is nonzero. We shall see that $SrTiO_3$ and $KMnF_3$ display behavior of this type.

In fluids the existence of a central component in the density fluctuations has been discussed in very similar terms by Mountain.[15] In this case the extra-low-frequency decay channel is provided by internal degrees of freedom of the fluid and introduced into Mountain's equations as a frequency-dependent viscosity of the form similar to Eq. (2).

Cowley pointed out that in a solid the qualitative structure which we postulate in the phonon self-energy might arise from the difference between collision-free and collision-dominated response.[12] For long-wavelength acoustic phonons the collision-dominated response is concerned essentially with the proper evaluation of the scattering diagram shown in Fig. 1(a), taking care to include the finite lifetime γ_T^{-1} of the pairs of thermal phonons with which the long-wavelength mode may interact.[16] With certain simplifying assumptions this leads to a self-energy of the form given by Eq. (2) with $\gamma = \gamma_T$. Shirane and Axe have used this as the basis of their discussion of the central peak which arises in conjunction with the acoustic instability in Nb_3Sn.[17] Simple momentum-conservation arguments suggest that the appropriate scattering process to study for a zone-boundary phonon mode is that shown in Fig. 1(b). It is not immediately obvious that the structure centered around $\omega = 0$ will be introduced by the self-energy contribution from this process, but Silberglitt has argued that this is indeed the case if one introduces the intermediate phonon states in a self-consistent manner.[18]

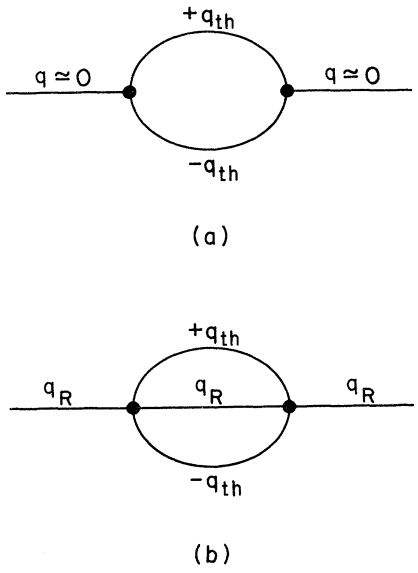

FIG. 1. Schematic representation of contribution to self-energy for (a) long-wavelength ($q \simeq 0$) phonons, (b) soft zone-boundary q_R phonons.

Feder[19] has pointed out that a central component would also be expected if there is a difference between adiabatic and isothermal response of the soft mode. The presence of a (temperature-dependent) condensed phonon mode guarantees such a difference below T_c, but Feder argues that such a difference exists above T_c, as well, if fluctuations are treated properly. In this model, γ would be some appropriate thermal diffusivity.

III. EXPERIMENTAL

The neutron-scattering measurements were made on a triple-axis spectrometer at the Brookhaven high-flux-beam reactor. The monochromator was a bent pyrolytic graphite (PG) crystal and the analyzer was a flat PG crystal. Soller slit systems with 20′ horizontal divergence were used to define the neutron path. The vertical divergence, determined by the natural collimator heights and the size of the crystal, was approximately 2°. The incident neutron energies E_0 used were 13.5 and 4.9 meV. Higher-order contamination was reduced to a negligible level by a PG filter[20] at the higher energy and a polycrystalline beryllium filter[21] at the lower energy. The contribution from the incoherent scattering was measured and subtracted from all the data. The spectrometer could be operated in a constant-Q (scanning-ω) or a constant-ω (scanning-Q) mode. The bulk of the data was obtained for constant-Q scans. The crystals were mounted in a nitrogen Dewar and tempera-

tures were controlled to better than 0.02 °K.

The $KMnF_3$ crystal was grown from a melt by means of a modified Czochralski method. The crystal was used in previous measurements and had a volume of 1 cm^3 and a 0.07° mosaic spread.[22] The transition temperature was measured by monitoring the intensity of the $\frac{1}{2}\frac{1}{2}\frac{3}{2}$ superlattice point as the temperature is lowered. At the transition temperature the intensity changes abruptly due to the first-order nature of the phase transition. T_c determined in this manner is (186.1 ± 0.5) °K. A hysteresis of less than 1 °K was observed between the cooling and heating curves of the intensity of the superlattice point.

Two crystals of $SrTiO_3$ were studied. One crystal supplied by National Lead Company[23] was grown by conventional flamed-fusion method and had a mosaic spread of 0.12°. It was cylindrical in shape, approximately 2 cm in diameter and 4.0 cm in length, with the cylindrical axis nearly parallel to [110]. The other crystal, supplied by Sanders Associates,[24] was grown by a top-seeded method and yielded essentially a strain-free crystal with a mosaic spread of only 0.03°. It was approximately cubic in shape with volume ~1 cm^3. The Sanders crystal had a brownish color whose origin has not yet been determined.

For $SrTiO_3$ the measurement of T_c proved to be difficult because of the narrow q and energy width of the critical scattering. Values of T_c were obtained by setting the spectrometer at a superlattice point and offsetting the energy by a small amount $\Delta\omega$ from $\omega = 0$. The intensity of the scattered neutrons was then monitored as a function of temperature. Measuring the maximum of this curve for several $\Delta\omega$ and extrapolating to $\omega = 0$ yielded values of the transition temperature. T_c for the National Lead Crystal is (105.0 ± 0.5) °K, which agrees well with recent EPR measurements on another crystal from the same supplier.[25] T_c as determined above for the nearly perfect Sanders crystal is (99.5 ± 0.3) °K. This value was also obtained by monitoring the intensity of the 222 Bragg point as the temperature was changed. Very near T_c there is a relief of extinction due to the formation of domains with a resultant increase in Bragg intensity. The result of these measurements is shown in Fig. 2. It is readily noted that T_c for the Sanders crystal is 5 °K lower than that measured for the National Lead crystal. This is not completely understood at present but might be attributed to the strain-free nature of the crystal. The majority of the $SrTiO_3$ measurements were made on the Sanders crystal because the extremely narrow sample mosaic simplified the resolution corrections.

Measurements were made on the crystals mounted in two different zones: [310] and [110]. These two zones enable us to measure the dispersion of the three lowest phonon branches relative to the R point.

IV. RESULTS

Energy scans at the R point of the Brillouin zone were made on $SrTiO_3$ and $KMnF_3$ to reveal both the phonon and the central peak. Figure 3 shows the results of these measurements for $SrTiO_3$ and $KMnF_3$ for $T - T_c = 15.2$ and 17.9 °K, respectively, with incident energy 4.9 meV. This figure reveals several important features. It shows unambiguously the existence of the central peak in $KMnF_3$ as well as in $SrTiO_3$. In the latter, the phonon peak (dotted line) is underdamped, whereas in $KMnF_3$ the phonon is well overdamped at this ΔT and appears as a broad line centered around $\omega = 0$. Sitting on top of this broad line is the narrow central peak. It also appears, rather qualitatively, that the central peak in $SrTiO_3$ is stronger than the central peak in $KMnF_3$. In addition, the linewidth of the central peak in both systems is that of the instrumental resolution. This sets an upper limit on the value of the energy linewidth of the central component: $\gamma < 0.02$ meV ($= 0.16$ cm^{-1} $= 4.8 \times 10^9$ Hz).

Representative temperature-dependent spectra for $SrTiO_3$ are shown in Fig. 4. The left-hand side of the figure shows how the frequency of the soft mode decreases and eventually merges into a broad peak centered around $\omega = 0$ for T very close to T_c. The right-hand side shows only the divergent central component. It is obvious that the in-

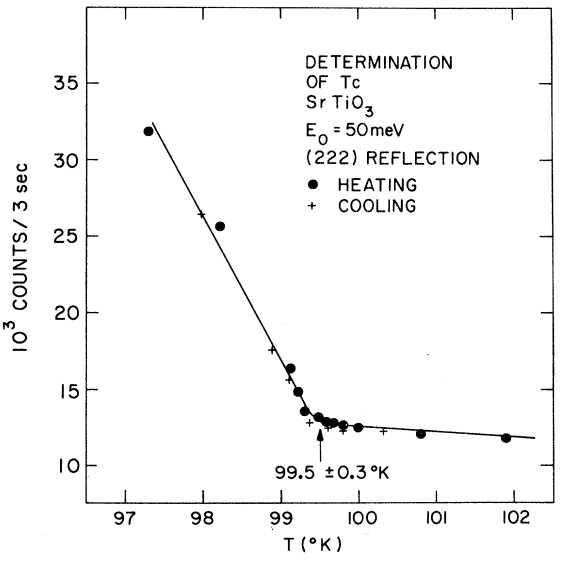

FIG. 2. Determination of the transition temperature of the Sanders $SrTiO_3$ crystal by monitoring the intensity of the neutrons elastically scattered from the (222) Bragg peak. The increase in intensity at T_c is due to relief of extinction as domains are created.

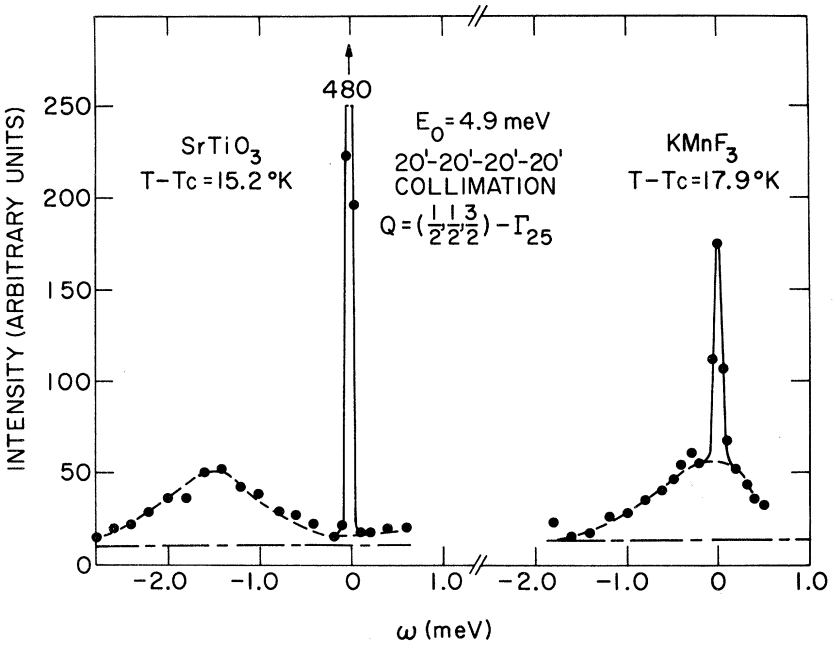

FIG. 3. Scattered-neutron spectra of $SrTiO_3$ and $KMnF_3$ at $T-T_c$ = 15.2 and 17.9 °K, respectively. The dotted line corresponds to the phonon peak and the solid line to the central component. The dashed line corresponds to level of room background. All incoherent scattering has been subtracted.

tensity of the central component is diverging quite rapidly as $T \to T_c$. The temperature-dependent spectra of $KMnF_3$ in Fig. 5 show the narrow central component superimposed upon the broader overdamped phonon. As $T \to T_c$, the overdamped phonon peak becomes narrower in energy and the intensity of the central component diverges. Because the phonon and the central-component contributions to the observed intensities are not clearly separated, the data analysis for $KMnF_3$ is greatly complicated. Thus in the remainder of the paper we refer mainly to the $SrTiO_3$ data.

Figures 3 and 4 also show that the relative linewidths of the phonon and the central peak are dramatically different. Since we are concerned with the total observed intensity $[S(\vec{q}, \omega)_{cent} + S(\vec{q}, \omega)_{side}]$ resolution-function corrections are required. The importance of these corrections can be visualized with the aid of Fig. 6, which schematically shows a cross section corresponding to a phonon dispersion surface, some additional cross section around $\omega = 0$, and the resolution ellipse drawn to scale

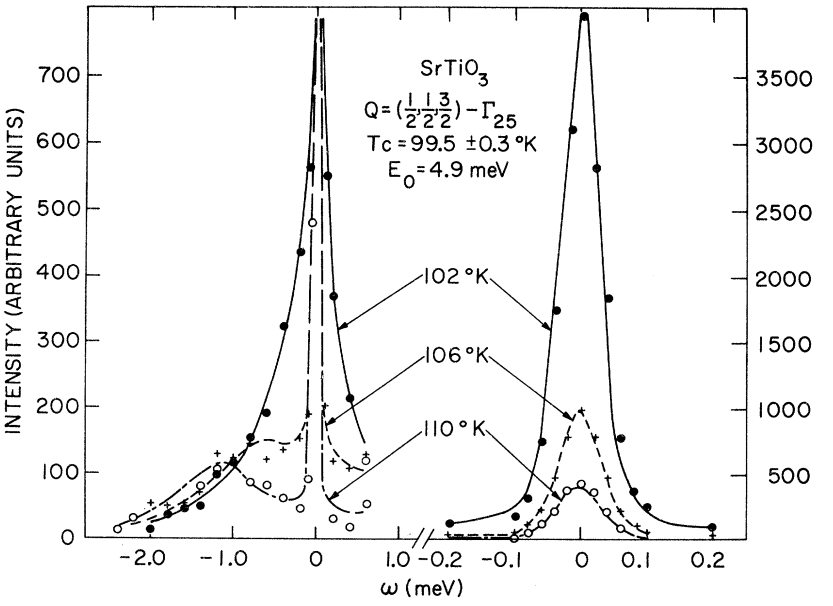

FIG. 4. Scattered-neutron spectra of $SrTiO_3$ at several temperatures. The left-hand side shows the soft-mode behavior of the phonon; the right-hand side shows the divergence of the central peak.

for 5 meV, with 20′ horizontal collimation. A constant-Q scan moves the resolution function parallel to the energy axis through the dispersion surfaces and the cross section at $\omega = 0$. For a particular setting of the spectrometer $(\vec{q}_0, \omega_0)$ the observed neutron intensity $I(\vec{q}_0, \omega_0)$ is proportional to the convolution of the scattering cross section with the resolution function of the apparatus:

$$I(\vec{q}_0, \omega_0) = A \iint \frac{d^2\sigma}{d\Omega\, d\omega} R(\vec{q} - \vec{q}_0, \omega - \omega_0)\, d\vec{q}\, d\omega \,, \tag{9}$$

where

$$\frac{d^2\sigma}{d\Omega\, d\omega} = \frac{k_f}{k_i} |F_{in}(\vec{Q})|^2 S(\vec{q}, \omega)$$

and $R(\vec{q} - \vec{q}_0, \omega - \omega_0)$ is the four-dimensional resolution function for a triple-axis spectrometer which has been discussed in detail by Cooper and Nathans.[26] The quantity A is a normalization constant containing instrumental parameters, k_i and k_f are the initial and final values of the wave vector of the neutrons, and $F_{in}(Q)$ is the inelastic structure factor for a particular mode at $\vec{Q} = \vec{q} + 2\pi\vec{\tau}$ ($\vec{\tau} \equiv$ reciprocal lattice vector).

Since the phonon dispersion surfaces are continuous in q within the Brillouin zone, they will completely fill the resolution function. But, since the additional cross section around $\omega = 0$ has a limited q extension, it will only fill a portion of the resolution function. Thus the weight factors determined by the resolution function are different for the phonon part and for the central component, and a comparison of the observed respective intensity components can lead to erroneous conclusions. In order to perform the proper resolution corrections, the full $\vec{q}$ dependence of $S(\vec{q}, \omega)$ has to be known. Since the phonon linewidth has almost no q dependence, we assume Γ_0 is independent of q. The assumption of γ being q independent will not affect our results. Because of the lack of any theoretical guide, we shall also assume δ^2 to be independent of q. If this is shown not to be the case, the results presented below will have to be modified. On the basis of the above assumptions, the entire q dependence of $S(\vec{q}, \omega)$ is included in the phonon frequency $\omega_\infty^2(\vec{q}, T)$. The resolution corrections are made at each temperature by analytically performing the convolution in Eq. (9) and then doing a least-squares refinement of the parameters in $S(\vec{q}, \omega)$ to obtain the best fit to the data.

$\omega_\infty^2(\vec{q})$ can be calculated by the method outlined in Ref. 8, where a truncated dynamical matrix is calculated for the three modes corresponding to rotations of the oxygen tetrahedra about the x, y, and z axes. As an approximation we neglect the smaller off-diagonal elements and obtain the fol-

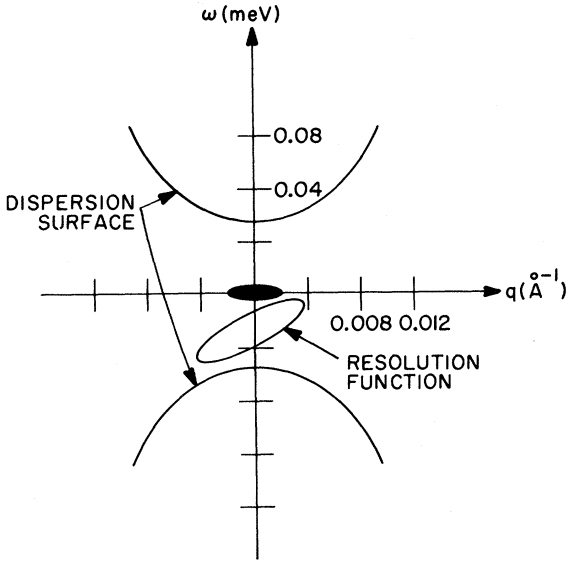

FIG. 6. ω-q plane schematically representing the phonon dispersion surface with an additional scattering cross section at $\omega = 0$. The resolution ellipse is drawn to scale for 5-meV incident neutron energy, 20′ horizontal collimation.

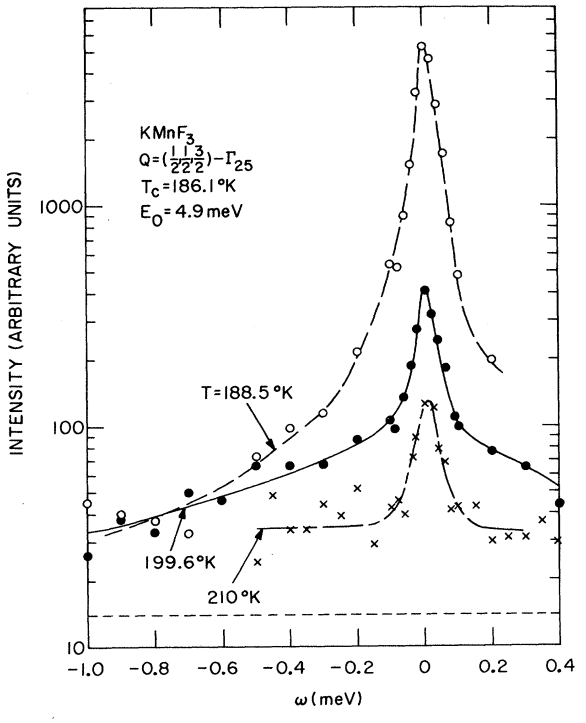

FIG. 5. Scattered-neutron spectra for $KMnF_3$ at several temperatures showing the narrow central peak superimposed upon the broader overdamped-phonon component. The dotted line represents the level of the room background. Note that the intensity scale is logarithmic. The curves are drawn as an aid to the eye.

lowing dispersion relations for the soft modes near q_R:

$$\omega_\infty^2(\vec{q}, T)_x = \omega_\infty^2(0, T) + \lambda_1 q_x^2 + \lambda_2(q_y^2 + q_z^2), \quad (10a)$$

$$\omega_\infty^2(\vec{q}, T)_y = \omega_\infty^2(0, T) + \lambda_1 q_y^2 + \lambda_2(q_x^2 + q_z^2), \quad (10b)$$

$$\omega_\infty^2(\vec{q}, T)_z = \omega_\infty^2(0, T) + \lambda_1 q_z^2 + \lambda_2(q_x^2 + q_y^2), \quad (10c)$$

where q_x, q_y, and q_z are the components of $\vec{q}$ measured from $\vec{q}_R$.

Two sets of values of λ_1 and λ_2 were tried in order to obtain the best fit to the data. The measured values of λ_1 and λ_2 along [001] and [110] are 300 and 3200 meV^2 Å^2, respectively. Because of the approximate nature of Eq. (10), $\lambda_1 = 500$ meV^2 Å^2 and $\lambda_2 = 1000$ meV^2 Å^2 gave a better fit to the zone-boundary-phonon profiles at high temperatures and were used in subsequent data analysis. The frequencies and intensities of the sidebands and the central peak far from T_c are relatively insensitive to the values of λ_1 and λ_2. However, close to T_c the intensities are sensitive to λ_1 and λ_2 and this sets a limit to the accuracy of our calculated parameters.

Included in the inelastic structure factor are the displacement vectors of the atoms. These are the eigenvectors associated with Eq. (10) and correspond to rotations of the oxygen tetrahedra about the x, y, and z axes, respectively.

Since the observed linewidth of the central peak was always resolution limited we chose a nominal value of γ' $[=\gamma(\omega_0^2/\omega_\infty^2)]$ to be such that it was always smaller than the energy resolution of the spectrometer. After a good fit was obtained γ' was allowed to vary. The fit was insensitive to γ' provided it was smaller than the instrumental resolution and larger than the mesh size required for the numerical folding.

The mesh size was such that the resolution function was divided into ten units from the center to $1/e^2$ intensity level along each of the four axes. Close to the transition temperature the results were checked by halving the size of the mesh in order to ascertain that there was little change in the deduced parameters and in the fit.

Once the parameters λ_1, λ_2, and γ were fixed the data were reduced in the following manner. In $SrTiO_3$ at $T - T_c > 6$ °K, the phonon is underdamped. One can neglect the center peak and fit only the phonon portion of the spectrum to obtain the constant A and the phonon parameters $\omega_\infty(0, T)$ and Γ_0. These three parameters are then held fixed and the central peak is fitted by adjusting δ. When the phonon becomes overdamped and the sidebands merge into an additional central component, we are able to keep A fixed and obtain $\omega_\infty^2(0)$ and Γ_0 by fitting to the phononlike wings of the central peaks. Again, once A, $\omega_\infty^2(0)$, and Γ_0 are known, δ is calculated from the central part of the peak alone.

Figure 7 shows the spectrum of $SrTiO_3$ at 110 °K. The circles represent the observed data and the solid line is the computer fit to the data via Eq. (9). The final values of the parameters for this fit are $\Gamma_0 = 0.88 \pm 0.1$ meV, $\delta^2 = 0.63 \pm 0.1$ meV^2, $\gamma < 0.02$ meV, $\omega_\infty^2(0) = 1.27 \pm 0.1$ meV^2. The dotted line is a plot of $S(q, \omega)$ given in Eq. (4) with an arbitrary normalization constant.

We see the importance of the resolution corrections by comparing the peak intensities of the "deconvolved" curve with the observed intensity. The phonon intensities are comparable but the intensity of the central peak for the deconvolved curve is over five times the observed peak intensity!

This method of treating the data proved reliable for $SrTiO_3$ because the phonon is underdamped to within 6 °K of T_c, enabling us to obtain the normalization parameter A. For $KMnF_3$ the phonon is overdamped for $T - T_c \leq 40$ °K and we cannot obtain a reliable value for the normalization parameter enabling us to find unique values of the remaining quantities. However, for large Γ_0 the cross section of Eq. (3) does produce a narrow central peak superimposed upon the broader phonon component. If we go to higher temperatures the phonon does become underdamped, but with the high resolution necessary to separate out the central peak there is too little intensity in the phonon peaks. However, we do observe the narrow central component superimposed upon the broader overdamped phonon component (Figs. 3 and 5). A rough estimate of the parameters from a trial fit to the data based upon the frequencies measured in Ref. 8 yields $\delta^2 = 0.27 \pm 0.1$ meV^2 and $\omega_\infty^2(0) = 2.64 \pm 0.4$ meV^2 for $T = 210$ °K. For $\Delta T > 15$ °K, the central component in $KMnF_3$ exhibits the same temperature dependence as observed in $SrTiO_3$ ($I_{cent} \sim T\omega_\infty^{-4} \sim T\omega_0^{-4}$).

Figure 8 shows the temperature dependence of δ^2, $\omega_\infty^2(0)$, and $\omega_0^2(0)$ for $SrTiO_3$ deduced from the observed neutron spectra by the method outlined above. These data are a combination of data taken at 4.9- and 13.5-meV incident energy. δ^2 is essentially constant ~0.9 meV^2, for $T > 125$ °K ($T - T_c \geq 25.5$ °K), and $\omega_0^2(0)$ and $\omega_\infty^2(0)$ have a linear behavior for $T - T_c > 15$ °K. The linear portion of the $\omega_\infty^2(0)$ curve extrapolates to zero frequency at $T_0 \approx 103$ °K, which is more than 3 °K above the independently measured T_c.

Figure 9 shows the temperature dependence of the three quantities on an expanded scale for temperatures near T_c. We observe that it is indeed the quantity $\omega_0^2(0)$ which approaches zero as $T \to T_c$ and explains the diverging intensity. The quantities ω_∞^2 and δ^2 decrease to finite and equal values at T_c: $\omega_\infty^2(T_c) = \delta^2(T_c) = 0.30 \pm 0.10$ meV.

Several constant $\omega = 0$ scans were made about the R point to measure the q width of the central peak.

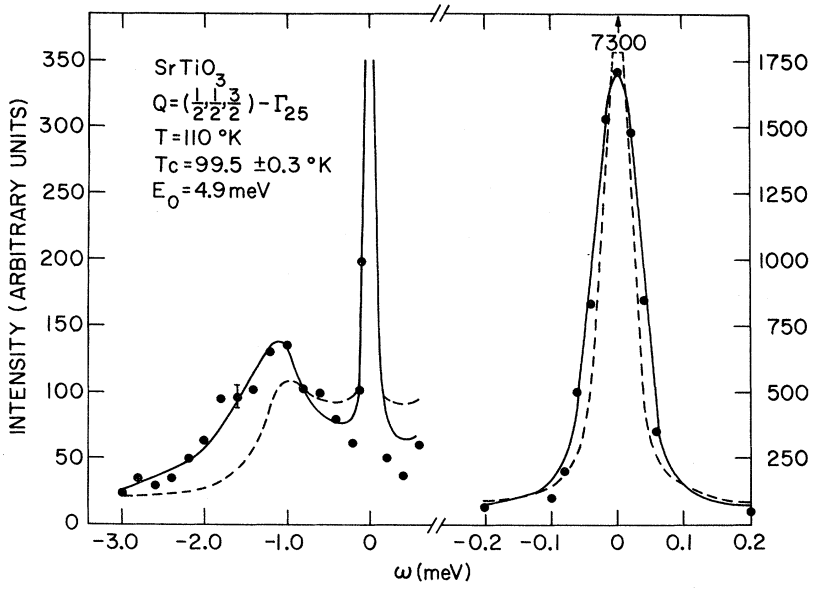

FIG. 7. Scattered-neutron spectrum of $SrTiO_3$ at $T = 110\,°K$. The circles are the observed data, the full line represents the fit of the data with Eq. (9); $\Gamma_0 = 0.88 \pm 0.1$ meV, $\delta^2 = 0.63 \pm 0.1$ meV^2, $\omega_\infty^2 = 1.27 \pm 0.1$ meV^2, $\lambda_1 = 500$ meV^2 Å^2, $\lambda_2 = 1000$ meV^2 Å^2. The dashed curve is a plot of $S(q, \omega)$ with the above parameters.

There is an increase in q width as $T - T_c$ increases. However, the observed q linewidth and its temperature dependence are much less than that reported earlier by Riste *et al.*[6,27] They reported a linewidth of $\Delta q_{1/2} = 0.10 \pm 0.04$ Å^{-1} at $T - T_c = 8.9\,°K$.

We observe, for the same ΔT, a linewidth of 0.02 ± 0.01 Å^{-1} prior to resolution corrections. This can be compared with a value for $\Delta q_{1/2}$ estimated from the expression for the integrated intensity of the central component [Eq. (8)] reasonably far from T_c:

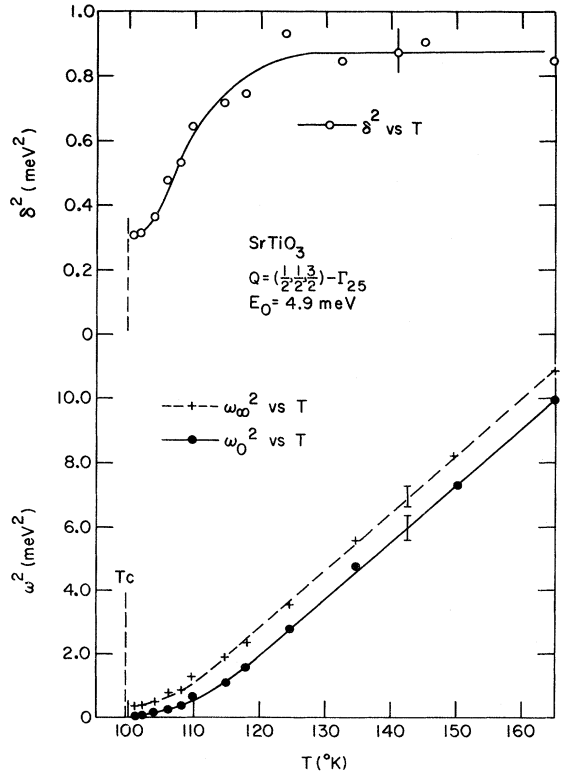

FIG. 8. δ^2, ω_∞^2, ω_0^2 vs T for $SrTiO_3$.

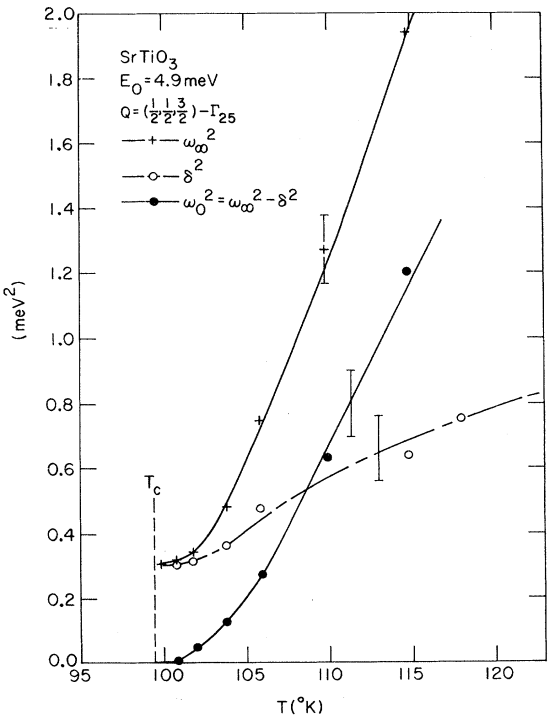

FIG. 9. ω_∞^2, δ^2, ω_0^2 vs T for $SrTiO_3$, close to transition temperature.

$$\Delta q_{1/2} \approx \frac{2[\omega_\infty^2(0)\omega_0^2(0)]}{\lambda^{1/2}[\omega_\infty^2(0)+\omega_0^2(0)]} ,$$

where we have used the assumption that δ^2 is q independent and λ is a combination of λ_1 and λ_2 given in Eq. (10). Knowing the expansion of $\omega_\infty^2(\vec{q})$ and using the calculated value δ^2, we find $\Delta q_{1/2} \sim 0.03$ Å^{-1} for $T - T_c \sim 9$ °K, which is in good agreement with our observed value.

In $KMnF_3$ the branch from the R-M point in the Brillouin zone has a very low frequency ($\lambda \simeq 10$ meV^2 Å^2), and a large anisotropy in the q width of the central component is expected. Preliminary observations revealed this anisotropy, although data were not corrected for the effects of the resolution function. A more detailed discussion of the q dependence of the central peak will be presented in a future publication.

Measurements were also made on the less perfect $SrTiO_3$ crystals obtained from the National Lead Company, and the observed neutron spectra exhibited a temperature-dependent behavior similar to that of the Sanders crystal. ω_∞^2 shows almost identical temperature-dependent behavior when the differences in T_c are considered, but the value of δ^2 is more difficult to deduce from the observed neutron intensities because of the difficulty in treating the sample mosaic. We do find that δ^2 is 35% lower in the National Lead crystal at $\Delta T = 15$ °K, which, provided we have correctly considered the sample mosaic in the fitting procedure, is outside of experimental error.

V. DISCUSSION

In Fig. 8 we observe that $\omega_\infty^2(T)$ is linear with temperature for $65\ ^\circ\mathrm{K} > T - T_c > 10\ ^\circ\mathrm{K}$. This is in agreement with the previous neutron study of the soft mode in $SrTiO_3$.[4,28,29] In fact, if we consider our measurements of the soft mode in the National Lead crystal the temperature dependence of the frequency can be written

$$\omega_\infty^2(0, T) = a(T - T_0)$$

in the temperature range $10\ ^\circ\mathrm{K} < T - T_0 < 180\ ^\circ\mathrm{K}$ with $a = 0.19$ meV^2 and $T_0 = 107.1$ °K, which is in close agreement with the values obtained in Refs. 4, 28, and 29. By an independent method we measured the transition temperature $T_c = 105.0 \pm 0.5$ °K, which is in agreement with T_c measured by other experimenters on crystals from the same supplier.[6,25] This value of T_c is over 2 °K lower than T_0. Likewise, in the Sanders crystal the phonon frequency can be fit by the same formula with $a = 0.18$ meV^2 and $T_0 = 103.5$ °K, although $T_c = 99.5$ °K. It is thus obvious that $\omega_\infty^2(0, T)$ deviates from a linear temperature behavior for $(T - T_c) < 10$ °K. The existing theory[30] which treats the temperature dependence of the soft mode for $T > T_c$ considers a model Hamiltonian within the framework of the mean-field theory and predicts a linear temperature dependence of $\omega_\infty^2(T)$ for $T - T_c < 100$ °K. This is consistent with the data for $100\ ^\circ\mathrm{K} > T - T_c > 10\ ^\circ\mathrm{K}$ but fails to explain the deviation from mean-field behavior observed for $T - T_c < 10$ °K.

The temperature dependence of δ^2 also shows an interesting behavior. For $T - T_c > 25$ °K, δ^2 has a constant value ~ 0.9 meV. At lower temperatures δ^2 decreases but then levels off to a limiting value at T_c. The behavior is clearly not monotonic with temperature and is influenced by the temperature dependence of the soft mode.

Since the intensity of the central component diverges at T_c, $\omega_0^2(T_c) = \omega_\infty^2(T_c) - \delta^2(T_c)$ is expected to go to zero, implying that $\omega_\infty^2(T_c) = \delta^2(T_c)$. This is observed in Fig. 9, where it is seen that $\omega_\infty^2(T_c) = \delta^2(T_c) = 0.3 \pm 0.1$ meV^2. In Silberglitt's discussion of the self-energy corrections for $SrTiO_3$ he estimated a value $\omega_\infty^2(T_c) = \delta^2(T_c) = 0.1$ meV^2, which is in remarkably close agreement to our observed values.[18]

Since $\omega_0^2(q, T)$ is proportional to the inverse static susceptibility the exponent governing the temperature behavior of $\omega_0^2(0, T)$ is the critical exponent[31] γ: $\omega_0^2 \sim (T - T_c)^\gamma$. However, a single exponent does not satisfactorily fit our results over the entire temperature range studied. Because of the uncertainty in T_c and the difficulty in performing resolution corrections close to T_c, our measurements of ω_0^2 are valid for $T - T_c > 1.3$ °K. This does not provide sufficient temperature range close to T_c to justifiably set a value for γ. We can speak in a semiquantitative manner and say that, for $1.3\ ^\circ\mathrm{K} < T - T_c < 10\ ^\circ\mathrm{K}$, γ has a value between 1.5 and 2.5, which is larger than the mean-field prediction of $\gamma = 1$.[31]

In light of the present results on $KmnF_3$ we may now reinterpret the anomalous soft-mode linewidth results reported by Gesi *et al.*[8] Because this study was carried out with low resolution no separation of the broad sideband and narrow central component was evident. The observed line shape was represented in a reasonable fashion by the overdamped-harmonic-oscillator form, Eq. (7), alone. They found, contrary to the simplest theoretical expectations, that the resulting Γ_0 was strongly temperature dependent. The present higher-resolution study has made clear that the unexpected behavior results not from a temperature-dependent $\Gamma_0(T)$, but rather from a frequency dependence of the soft-mode damping. In fact, the normal (high-frequency) part of the damping is indeed relatively temperature independent, in agreement with theoretical estimates.

It would be most interesting to study the behavior of the critical scattering below T_c. However,

because of the extremely narrow q width and because the zone boundary becomes the zone center in the tetragonal phase, it is difficult to separate the critical scattering from the elastic Bragg scattering. It is hoped that the high energy and the high-q resolution associated with inelastic light and x-ray scattering can further clarify the nature of the critical scattering below T_c.

ACKNOWLEDGMENTS

The authors are indebted to M. Blume, J. Feder, P. Hohenberg, K. Otnes, E. Pytte, E. Samuelsen, and R. Silberglitt for the invaluable discussions. We also thank J. Als-Nielsen for the computer program which was used in performing the resolution-function corrections.

---

†Work performed under the auspices of the U. S. Atomic Energy Commission and NATO Research Grant.

*Visiting scientist at Brookhaven National Laboratory, Summer 1971.

[1]*Structural Phase Transitions and Soft Modes*, edited by E. J. Samuelsen, E. Andersen, and J. Feder (Universtetsforlaget, Oslo, Norway, 1971).

[2]P. W. Anderson, in *Fizika Dielectrikov*, edited by G. I. Skanavi (Academy of Sciences, USSR, Moscow, 1960); W. Cochran, Advan. Phys. 9, 387 (1960).

[3]P. A. Fleury, J. F. Scott, and J. M. Worlock, Phys. Rev. Letters 21, 16 (1968).

[4]G. Shirane and Y. Yamada, Phys. Rev. 177, 858 (1969).

[5]K. A. Müller and W. Berlinger, Phys. Rev. Letters 26, 13 (1971).

[6]T. Riste, E. J. Samuelsen, K. Otnes, and J. Feder, Solid State Commun. 9, 1455 (1971).

[7]A preliminary report is given in *Proceedings of the International Conference on Phonons, Rennes, France*, 1971, edited by M. A. Nusimovici (Flammarion, Paris, 1971), p. 155.

[8]K. Gesi, J. D. Axe, G. Shirane, and A. Linz, Phys. Rev. B 5, 1933 (1972).

[9]R. Comès, F. Denoyer, L. Deschamps, and M. Lambert, Phys. Letters 34A, 65 (1971).

[10]V. J. Minkiewicz and G. Shirane, J. Phys. Soc. Japan 26, 674 (1969); V. J. Minkiewicz, Y. Fujii, and Y. Yamada, *ibid.* 28, 443 (1970).

[11]K. Tani, J. Phys. Soc. Japan 26, 93 (1969).

[12]R. A. Cowley, J. Phys. Soc. Japan Suppl. 28, S239 (1970).

[13]See, for example, R. A. Cowley, Advan. Phys. 12, 421 (1963). Equation (1) omits nondiagonal self-energy terms which can cause interference effects with other normal modes.

[14]F. Schwabl [Phys. Rev. Letters 21, 500 (1972)] has discussed the effect of a self-energy of the form of Eq. (2) on the behavior of ultrasonic attenuation in $SrTiO_3$.

[15]R. D. Mountain, J. Res. Natl. Bur. Std. (U. S.) A70, 207 (1966).

[16]B. D. Silverman [Solid State Commun. 10, 311 (1972)] invoked similar arguments in discussing soft-mode–linewidth divergence in $PbTiO_3$.

[17]G. Shirane and J. D. Axe, Phys. Rev. Letters 27, 1803 (1971).

[18]R. Silberglitt, Solid State Commun. 11, 247 (1972).

[19]J. Feder, Solid State Commun. 9, 2021 (1971).

[20]G. Shirane and V. J. Minkiewicz, Nucl. Instr. Methods 89, 109 (1970).

[21]B. N. Brockhouse, in *Inelastic Scattering of Neutrons in Solids and Liquids* (International Atomic Energy Agency, Vienna, 1961), p. 113.

[22]G. Shirane, V. J. Minkiewicz, and A. Linz, Solid State Commun. 8, 1941 (1970).

[23]National Lead Company, P. O. Box 58, South Amboy, N. J. 08879.

[24]Sanders Associates, Electro-Optics Div., 95 Canal St., Nashua, N. H.

[25]K. A. Müller, in Ref. 1, pp. 61ff.

[26]M. J. Cooper and R. Nathans, Acta Cryst. 23, 357 (1967).

[27]T. Riste, E. J. Samuelsen, and K. Otnes, in Ref. 1, pp. 395ff.

[28]R. A. Cowley, W. J. L. Buyers, and G. Dolling, Solid State Commun. 7, 181 (1969).

[29]K. Otnes, T. Riste, G. Shirane, and J. Feder, Solid State Commun. 9, 1103 (1971).

[30]E. Pytte and J. Feder, Phys. Rev. 187, 1077 (1969).

[31]H. E. Stanley, *Introduction to Phase Transitions and Critical Phenomena* (Oxford U. P., New York, 1971).